Contents lists available at ScienceDirect

Solid State Communications

journal homepage: www.elsevier.com/locate/ssc

Lithium transport investigation in Li$_x$FeSiO$_4$: A promising cathode material

Rafael B. Araujo [a,b,c,*], Ralph H. Scheicher [b], J.S. de Almeida [a], A. Ferreira da Silva [a], Rajeev Ahuja [b,c]

[a] Instituto de Física, Universidade Federal da Bahia, Campus Universitário de Ondina, 40210-340 Salvador, Bahia, Brazil
[b] Condensed Matter Theory Group, Department of Physics and Astronomy, Box 516, Uppsala University, SE-751 20 Uppsala, Sweden
[c] Applied Materials Physics, Department of Materials Science and Engineering, Royal Institute of Technology (KTH), SE-100 44 Stockholm, Sweden

ARTICLE INFO

ABSTRACT

In this paper we investigate lithium mobility in both Li$_2$FeSiO$_4$ and its half-lithiated state LiFeSiO$_4$ considering an orthorhombic crystal structure. We find that the calculated activation energy of Li$^+$ ions hopping between adjacent equilibrium sites predicts two least hindered diffusion pathways in both materials. One of them is along the [100] direction characterizing an ionic diffusion in a straight line and the other follows a zig-zag way between the Fe–Si–O layers. We also show that diffusion of Li$^+$ ions in the half-lithiated structure follows the same behavior as in the lithiated structure. As a whole, the activation energies for the investigated compounds present a greater value compared with the activation energies in currently used materials such as LiFePO$_4$. The results were calculated in the framework of density functional theory in conjunction with the climbing image nudged elastic band method. The Hubbard term was added to the Kohn–Sham Hamiltonian to overcome the delocalization problem of d electrons. Furthermore, the diffusion coefficients were calculated for both structures considering temperatures ranging from 300 to 700 K.

© 2013 Elsevier Ltd. All rights reserved.

1. Introduction

Lithium iron silicate (Li$_2$FeSiO$_4$) has appeared in the last years as an alternative cathode material in Li-ion batteries since it exhibits low production cost, good performance and non-toxicity [1]. Li$_2$FeSiO$_4$ was first synthesized and characterized by Nytén et al. [1] in an orthorhombic lattice with $Pmn2_1$ space group. Numerous experiments [1–12] and theoretical calculations [13–20] have been carried out on this material, showing advantages such as environmental benignity, high cycle stability, and a theoretical capacity as high as 166 mAh g^{-1}.

The performance of batteries is also closely related to the ionic conductivity of the materials. In that sense, the investigation of lithium migration mechanisms becomes an important tool in Li-batteries field. For instance, the framework of the Density Functional Theory (DFT) was used in Ref. [21] to investigate lithium diffusion considering Li$_2$FeSiO$_4$ as a cathode material in $Pmn2_1$ crystal symmetry. They have found a diffusion of Li$^+$ ions proceeding along the [100] and [001] directions exhibiting a two-dimensional Li$^+$ ion diffusion character with activation energy barriers of 0.84

and 0.88 eV, respectively. However, the authors did not investigate the diffusion process in the half-lithiated crystal structure. It is of utmost importance to understand the lithium migration mechanisms in the half-lithiated structure as well, since the performance of the battery depends on the lithium migration process in both systems. The present work aims to investigate the migration mechanisms of Li$^+$ ions in orthorhombic Li$_2$FeSiO$_4$ and in its half-lithiated phase (LiFeSiO$_4$). We compare our revealed results for the energy barriers with the reported ones in Ref. [21] and, furthermore, we show the diffusion mechanisms in the LiFeSiO$_4$ crystal structure. This work was carried out by using DFT together with the climbing Nudged Elastic Band (cNEB) method to predict the energy barriers encountered by the Li$^+$ ions. To overcome the well known delocalization problem of d electrons in transition metal oxides associated with the current DFT methods such as the local density approximation (LDA) or the generalized gradient approximation (GGA) we have added the Hubbard term to the Kohn–Sham Hamiltonian.

This paper will be organized as follows. In Section 2, we present the theoretical background and the computational details along with the computational parameters used in this work. The structural stability of Li$_2$FeSiO$_4$ as well as that of LiFeSiO$_4$ was studied in detail in Section 3. We present the lithium migration results and diffusion coefficients in Sections 4 and 5. In Section 6 we conclude with a brief summary of the reported results provided by our *ab initio* calculations.

* Corresponding author at: Universidade Federal da Bahia, Instituto de Física, Salvador, Bahia, Brazil. Tel.: +55 71 3283 6615.
E-mail addresses: rafael.barros@physics.uu.se, rafaelbna@gmail.com (R.B. Araujo), rajeev.ahuja@fysik.uu.se (R. Ahuja).

2. Computational details

We performed density functional theory (DFT) *ab initio* calculations based on the projector augmented wave (PAW) method as implemented in the Vienna Ab initio Simulation Package (VASP) [22,23]. The exchange and correlation terms are treated within the spin-polarized generalized gradient approximation (GGA) in the Perdew and Wang parametrization (PW91) [24]. To take into account the localization of d electrons in the transition metal ions in these materials, we have also included the Hubbard term in the Kohn–Sham Hamiltonian following the approach by Dudarev et al. [25]. We have used $U=5$ eV, which was shown by previous investigations [14,16,21,26–28] to be a suitable value for these systems to reproduce features such as open circuit voltage and band gap. The energy cut-off for the wave function expansion was set to 400 eV. Integrals were calculated over the Brillouin zone by the Gaussian smearing method with only one k point (Γ point) due to the large size of the supercell. From our total-energy calculation we have found that the antiferromagnetic (AFM) state is lower in energy compared to both ferromagnetic (FM) and paramagnetic (PM) states. Furthermore, it was demonstrated in previous studies that the magnetic ordering does not affect the diffusion mechanisms [21]. Therefore, we have chosen to work with the AFM state which has also helped to overcome convergence issues on the cNEB calculations.

The Li^+ diffusion barrier heights in Li_2FeSiO_4 and $LiFeSiO_4$ crystal structures were investigated with the cNEB method [29,30] in a $2a \times 2b \times 2c$ supercell containing 16 formula units corresponding to 128 atoms (lithiated system) and 112 atoms (delithiated systems), respectively. The large supercell dimensions ensure that the atoms are separated from their periodic image, providing a more accurate answer for the activation barrier in the diluted limit. A lithium vacancy was created in the supercell of Li_2FeSiO_4, while an extra lithium atom was added to the supercell of $LiFeSiO_4$ in order to enable our study of Li ion diffusion. By adding or removing a Li atom (Li^+ and e^-) in the delithiated and lithiated systems we are properly modeling the oxide-reduction reaction that occurs in the cathode during the charging and discharging processes of the battery. To determine the minimum energy path (MEP) through the cNEB method, six replicas of the system were created, in each of which the diffusing Li atom was moved by equidistant steps to positions between the initial and final states for the path obtained from linear interpolation.

3. Crystal structure

The crystal structure of orthorhombic Li_2FeSiO_4 was taken from Ref. [13]. It consists of a lattice built up from infinite conjugated layers of composite $SiFeO_4$ linked through the LiO_4 tetrahedra, with each Li, Fe, Si located in the center of the tetrahedra formed by four oxygen atoms. Furthermore, the Li^+ ions are occupying tetrahedra sites between the FeO_4–SiO_4 where the tetrahedra point in the same directions. One can observe from Fig. 1 that when we create the vacancy there exist many Li^+ ions near enough to hop, contributing to the diffusion process. However, the conditions for such a jump are much better for certain Li^+ ions than for others, and therefore result in much smaller activation energies. For Li_2FeSiO_4 two migration pathways were identified. Fig. 1(a) is showing the Pathway A which is characterized by a zig-zag trajectory in the bc plane with Li^+ ions moving between the Si–Fe–O layers. Fig. 1(b) is presenting the Pathway B. It is characterized by a linear motion of Li^+ ions along the a-axis. Another pathway that we could take into account is one where the Li^+ ions cross the FeO_4–SiO_4. However, the electrostatic repulsion felt by a Li^+ ion in that case should be rather large. Therefore,
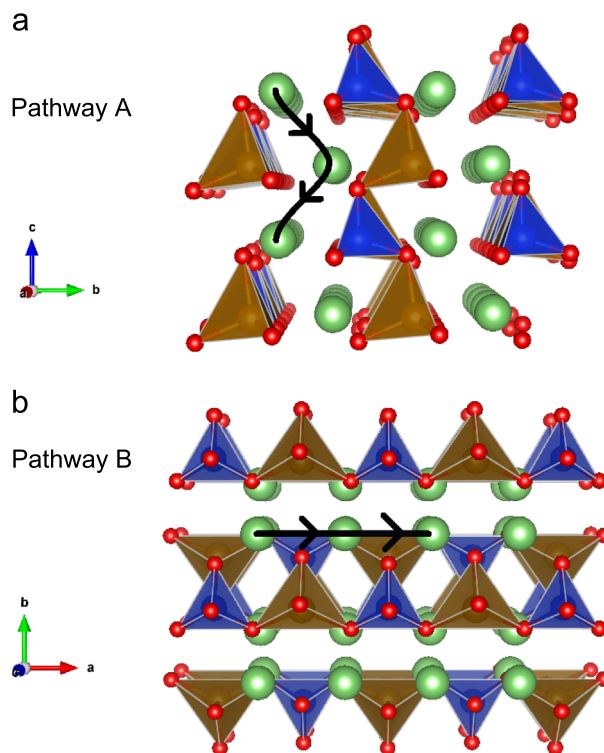

Fig. 1. (Color online) Diffusion pathways of Li^+ ions in Li_2FeSiO_4 crystal structure. (a) Pathway A, lithium ions moving in a zig-zag trajectory. (b) Pathway B, linear diffusion of the lithium ions along the a-axis. Here, brown tetrahedra are formed by Fe and O atoms. Blue tetrahedra are formed by Si and O atoms. Li ions are depicted in green.

we have decided to investigate only the Pathways A and B for the lithium migration.

4. Lithium migration results

4.1. Lithiated structure

Fig. 2 is showing the results of the cNEB calculations of the two selected pathways in the Li_2FeSiO_4 crystal structure. The hopping distance in the Pathway A (left panel of Fig. 2) is 3.70 Å between the neighboring equilibrium sites. The corresponding activation energy is 0.98 eV. The right panel of Fig. 2 is representing the activation energy predicted for Li^+ diffusion in the Pathway B. The observed hop distance for this path is 3.74 Å and it displays an activation barrier of 0.88 eV. Comparing the calculated values of the energy barriers with regard to the chosen paths it is noticed that Pathway B presents a lower value. Analyzing the Pathway A one can see that in the transition state the lithium ion is electrostatically repelled from the closest two Fe atoms and two Si atoms. On the other hand, the Li^+ in the transition state considering the Pathway B reveals just one Fe atom and one Si atom close enough to interfere in the hopping process. Therefore, the electrostatic repulsion acting on the Li^+ ion in the Pathway B is lower resulting in a lower energy barrier as well. These results are in agreement with the reported lithium activation energies in Ref. [21]. The authors of that study have shown that the most probable pathways in the Li_2FeSiO_4 crystal structure are a straight hop along the [100] direction and a zig-zag hop within the (001) plane with activation energy barriers of 0.84 eV and 0.88 eV, respectively. The predicted energy barriers value in Ref. [21] are somewhat different from our results since we found 0.88 eV for lithium migration in the straight pathway (Pathaway B) and 0.98 eV for the zig-zag
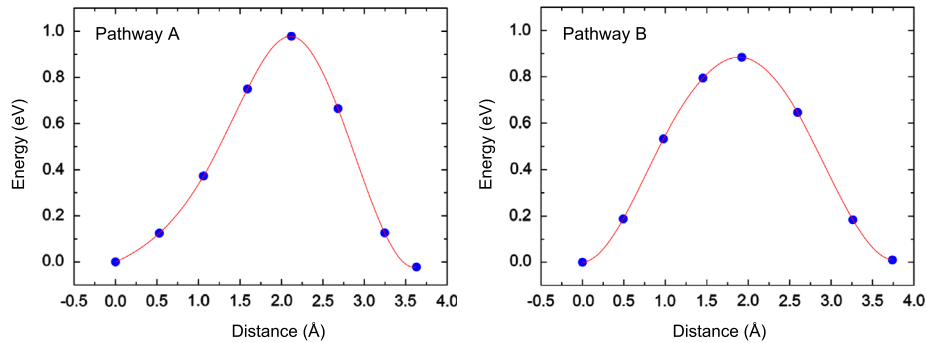
Fig. 2. (Color online) Lithium ion migration in orthorhombic Li_2FeSiO_4 as obtained from cNEB method. The red line is just to give a visual help of the sequence of images. Blue symbols represent calculated data points. Here, we present the calculations carried out for Pathway A and for Pathway B.

pathway (Pathway A). However, even with this difference in the activation energy value both of us are predicting a two-dimensional lithium diffusion in Li_2FeSiO_4. Moreover, we display the same possible pathways as the most probable ones for the lithium hopping in this material.

The results for the energy barrier reported in Ref. [19], which has performed cNEB calculations in Li_2FeSiO_4 with the GGA approach, reveal a value of 0.74 eV for Pathway A and 0.83 eV for Pathway B. That difference could be a result of the Hubbard term inclusion into the Kohn–Sham Hamiltonian. The usage of the GGA+U scheme leads to a change of the electronic structure, reflecting the ground state crystal structure and, finally, leading to a different value in the activation energy. That difference compared to our results is of around 25% and 6% in Paths A and B, respectively. The most important point to be observed in this comparison between the results reported in Ref. [19] and the calculations performed here is that there occurs a change in the most probable pathway for the lithium migration. Here, it was revealed a lower activation energy for Pathway B, characterizing a one-dimensional diffusion through the a-axis while Ref. [19] has predicted the Pathway A as the most probable one leading to a zig-zag lithium diffusion.

The prediction of the lithium diffusion activation energies in Li_2FeSiO_4 with monoclinic structure was first reported in Ref. [31]. The cNEB calculations reveal a zig-zag motion between the FeSiO layers as the most probable one with an activation energy of 0.83 eV [31]. Here, our results predict the diffusion along the a-axis and with an activation energy amounting to 0.88 eV. It means that Li_2FeSiO_4 with monoclinic structure presents a faster ionic diffusion than Li_2FeSiO_4 in the orthorhombic phase.

4.2. Half-lithiated structure

To obtain a better understanding of the lithium diffusion mechanisms in the lattice of the delithiated crystal state we have taken the $LiFeSiO_4$ crystal structure in the $Pmn2_1$ symmetry from Ref. [13] and created a supercell of $2a \times 2b \times 2c$. After this procedure, a defect was added into the supercell lattice, i.e., we have introduced a new Li atom to correctly describe the reduction process that occurs in the discharging of the battery. A new optimization process was carried out and as a result we obtained the lattice parameters $2a=12.10$ Å, $2b=10.87$ Å, and $2c=9.80$ Å for the supercell. The diffusion pathways for the half-lithiated structure were chosen following the same criteria used in the lithiated case. Fig. 3 is showing the selected pathways. The only difference in comparison with the chosen pathways of the lithiated system is that here we divided each path into two parts. We carried out cNEB calculations to predict the activation energy of the Li ion hop from site 1 to site 2 and, in sequence, we performed the same calculation to find the activation energy of the hop from site 2 to site 3, as illustrated in Fig. 3.
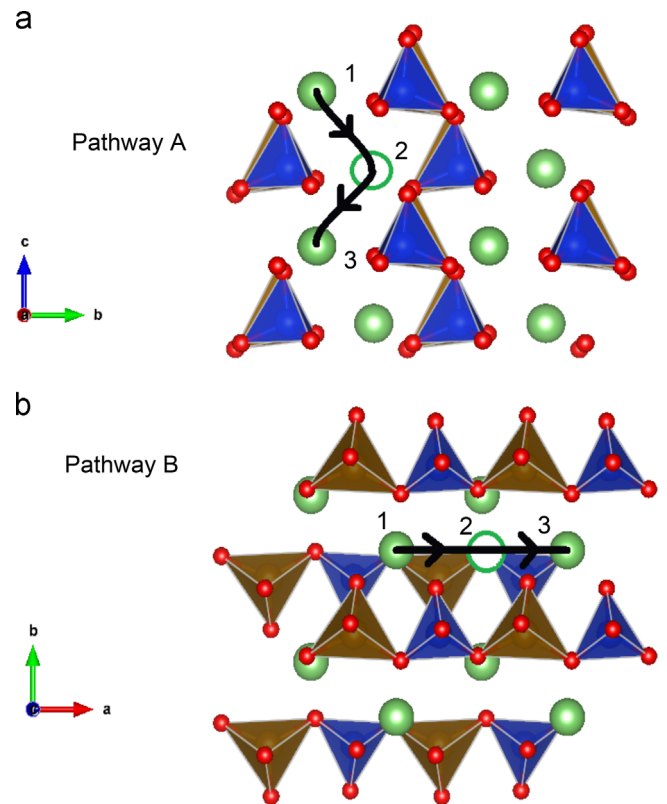

Fig. 3. (Color online) Crystal structures and diffusion pathways of the Li^+ ions in $LiFePO_4$. The numbers 1, 2 and 3 are representing the equilibrium Li^+ sites in the crystal structure. The sites 1 and 3 are equivalents while site 2 (represented by an open green circumference) is a non-equivalent site. (a) Pathway A, lithium ions in a zig-zag trajectory. (b) Pathway B, linear diffusion of the lithium ions along the a-axis. Here, brown tetrahedra are formed by Fe and O atoms. Blue tetrahedra are formed by Si and O atoms.

Fig. 4 is showing the activation energy of the Pathways A and B in the orthorhombic crystal structure of $LiFeSiO_4$. The presented hopping distance for both pathways is 7.95 Å and 7.58 Å, respectively. The energy barrier for Pathway A is 1.05 eV in the case of Li^+ hopping between the equilibrium sites 1 and 2. Moreover, the activation energy displayed for the hop between the equilibrium sites 2 and 3 is 1.00 eV. As a whole the dominant activation energy of the Pathway A is 1.05 eV. The Pathway B is presenting an activation energy value of 0.85 eV and 0.90 eV to the hop sites 1 to 2 and 2 to 3, respectively. The dominant activation energy in this case would be 0.90 eV. Comparing both paths, it can be noticed that the Pathway B would be the most probable one. It describes an one-dimensional Li ion diffusion path along the a-axis just as predicted for the lithiated structure. We can observe an increase of
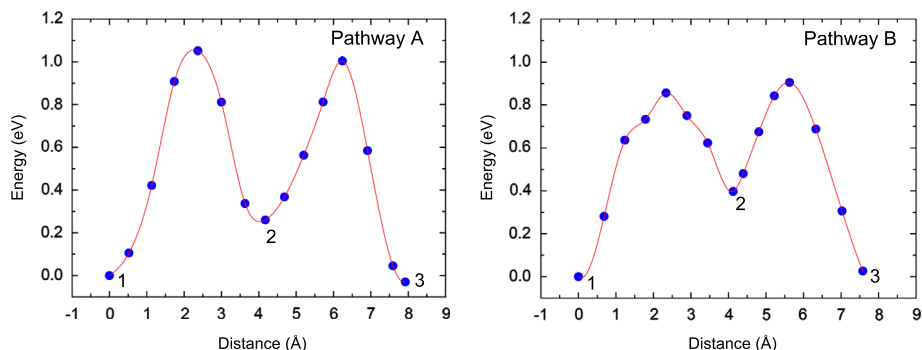
Fig. 4. (Color online) Lithium ion migration in orthorhombic LiFeSiO$_4$ as obtained from cNEB method. The red line is just to give a visual help of the sequence of images. Blue symbols represent calculated data points. Here, we present the calculation carried out for the Pathway A and for the Pathway B. The values 1, 2 and 3 are representing the equilibrium sites of the lithium ion.
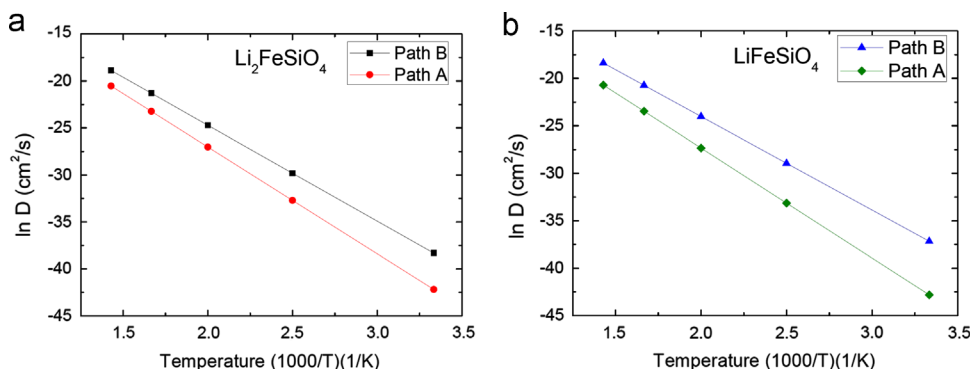

Fig. 5. (Color online) Natural logarithm of the diffusion coefficient against $1/T$ for the lithiated (a) and half-lithiated (b) systems in different possible pathways.

the activation energy in the most probable path of only 2% in comparison with the lithiated system.

The lithium diffusion results reported in Ref. [19] considering the GGA approach to the delithiated structure are displaying an activation energy of 0.97–1.05 eV in the Pathway A and 0.87 eV for Pathway B. Here, even with the adding of the Hubbard term, the results for the energy barriers show to be in reasonable agreement with Ref. [19]. Comparing the reported results of the activation energies in a monoclinic crystal structure ($P2_1$ symmetry) calculated in Ref. [19] and the results for the $Pmn2_1$ crystal symmetry reported here it was observed that the lithium diffusion would occur easily in the monoclinic crystal structure even in the delithiated state. It can be explained by the greater value of the volume in the unit cell of the $P2_1$ structure.

5. Diffusion coefficient

The lithium diffusion coefficient can be calculated as $D = d^2 \Gamma$, where d is the hopping distance and Γ is the hopping rate being defined in the transition state theory [32] as $\Gamma = \nu_0 \exp(-E_a/k_B T)$. In this case, E_a is the activation energy, k_B is the Boltzmann constant, T is the temperature, and ν_0 is the attempt frequency. Therefore the diffusion constant D can be written as

$$D = d^2 \nu_0 \exp\left(-\frac{E_a}{k_B T}\right) \tag{1}$$

All calculations for the diffusion coefficient were performed considering ν_0 about 10^{13} Hz, which is in the range of the phonon frequencies and consistent with typical values for the attempt frequency [33]. For the temperature we considered 300 K, 400 K, 500 K, 600 K, and 700 K. Fig. 5(a) and (b) summarizes all diffusion coefficients for both systems. Since we have plotted the natural logarithm of the diffusion coefficient against $1/T$, we can see

that the activation barrier is proportional to the slope of each straight line.

Analyzing the results for Li$_2$FeSiO$_4$ shown in Fig. 5(a) one can observe that the Pathway B reveals the highest value of the diffusion coefficients. This indicates a straight lithium migration with the diffusion to take place between the shortest linear Li sites. Pathway A also contributes to the lithium migration; however, it exhibits a higher activation barrier leading to a smaller value of the diffusion coefficient. The diffusion coefficient in the Li$_2$FeSiO$_4$ crystal structure is significantly lower than what was found for other common cathode materials at room temperature. For example, for the commercially used Li$_x$CoO$_2$ the diffusion coefficient has been found to be within the range of 10^{-13} to 10^{-7} cm^2/s at room temperature [33]. Fig. 5(b) summarizes the obtained results for the diffusion coefficient in the half-lithiated crystal structure. This case reveals the same behavior as predicted for the lithiated system. Therefore, the lithium diffusion in the investigated compound appears to be two-dimensional with Li ions traveling through Pathways A and B.

6. Conclusion

In this paper, we studied different migration paths for lithium in the Li$_x$FeSiO$_4$ ($x=1,2$) crystal structure. We identified those which yield the lowest barrier and are thus most likely to contribute to the Li ion diffusion. Our results reveal that the most probable migration path in the lithiated system is the one in which Li ions follow a straight line between the Fe–Si–O layers (Pathway B). However, the activation barrier calculated for an alternative pathway with the Li$^+$ ions moving in a zig-zag way (Pathway A) is quite close to that for Pathway B, thus making it possible to consider that this path can also contribute to the Li ion migration. The diffusion of Li ions considering the delithiated structure followed the same

behavior displayed in the lithiated case. Therefore, our predictions reveal a two-dimensional lithium diffusion in the Li_xFeSiO_4 crystal structures. Finally, when comparing the diffusion coefficient in Li_2FeSiO_4 at room temperature, ranging from 10^{-20} cm^2/s up to 10^{-17} cm^2/s, with the diffusion coefficient in currently used materials typically ranging from 10^{-13} cm^2/s to 10^{-7} cm^2/s [33], it is seen clearly that Li_2FeSiO_4 can at the moment not provide better kinetics than the state-of-the-art materials. More work is thus needed to improve ion diffusion in this material.

Acknowledgments

References

[1] A. Nytén, A. Abouimrane, M. Armand, T. Gustafsson, J.O. Thomas, Electrochemistry Communications 7 (2005) 156.
[2] A. Nytén, S. Kamali, L. Häggström, T. Gustafsson, T.O. John, Journal of Materials Chemistry 16 (2006) 2266.
[3] R. Dominko, M. Bele, M. Gaberscek, A. Meden, M. Remskar, J. Jamnik, Electrochemistry Communications 8 (2006) 217.
[4] Z.L. Gong, Y.X. Li, Y. Yang, Electrochemical and Solid-State Letters 9 (2006) A542.
[5] K. Zaghib, A.A. Salah, N. Ravet, A. Mauger, F. Gendron, Julien, Journal of Power Sources 160 (2006) 1381.
[6] A. Nytén, M. Stjerndahl, R. Håkan, S. Hans, A. Michel, G. Torbjörn, E. Kristina, O.T. John, Journal of Materials Chemistry 16 (2006) 3483.
[7] R. Dominko, M. Bele, A. Kokalj, M. Gaberscek, J. Jamnik, Journal of Power Sources 174 (2007) 457.
[8] Z.L. Gong, Y.X. Li, Y. Yang, Journal of Power Sources 174 (2007) 524.
[9] Y.X. Li, Z.L. Gong, Y. Yang, Journal of Power Sources 174 (2007) 528.
[10] V.V. Politaev, A.A. Petrenko, V.B. Nalbandyan, B.S. Medvedev, E.S. Shvetsova, Journal of Solid State Chemistry 180 (2007) 1045.
[11] R. Dominko, D.E. Conte, D. Hanzel, M. Gaberscek, J. Jamnik, Journal of Power Sources 178 (2008) 842.
[12] R. Dominko, Journal of Power Sources 184 (2008) 462.
[13] P. Larsson, R. Ahuja, A. Nytén, T.O. Thomas, Electrochemistry Communications 8 (2006) 797.
[14] M.E. Arroyo-de Dompablo, M. Armand, J.M. Tarascon, U. Amador, Electrochemistry Communications 8 (2006) 1292.
[15] S.Q. Wu, J.H. Zhang, Z.Z. Zhu, Y. Yang, Current Applied Physics 7 (2007) 611.
[16] M.E. Arroyo-de Dompablo, R. Dominko, G.M. Gallardo-Amores, L. Dupont, G. Mali, H. Ehrenberg, J. Jamnik, E. Morán, Chemistry of Materials 20 (2008) 5574.
[17] M.E. Arroyo de Dompablo, J.M. Gallardo-Amores, J. García- Martínez, E. Morán, J.M. Tarascon, M. Armand, Solid State Ionics 179 (2008) 1758.
[18] S.Q. Wu, Z.Z. Zhu, Y. Yang, Z.F. Hou, Computational Materials Science 44 (2009) 1243.
[19] A. Liivat, J.O. Thomas, Solid State Ionics 192 (2011) 58.
[20] R.B. Araujo, R.H. Scheicher, J.S. de Almeida, A. Ferreira da Silva, R. Ahuja, First-principles investigation of Li ion diffusion in Li_2FeSiO_4, Solid State Ionics 247–248 (2013) 8–14.
[21] K.M. Bui, V.A. Dinh, T. Ohno, Applied Physics Express 5 (2012) 125802.
[22] G. Kresse, J. Hafner, Physical Review B 47 (1993) 558.
[23] G. Kresse, J. Hafner, Physical Review B 54 (1996) 11169.
[24] J.P. Perdew, J.A. Chevary, S.H. Vosko, K.A. Jackson, M.R. Pederson, D.J. Singh, C. Fiolhais, Physical Review B 46 (1992) 6671.
[25] S.L. Dudarev, G.A. Botton, S.Y. Savrasov, C.J. Humphreys, A.P. Sutton, Physical Review B 57 (1998) 1505.
[26] F. Zhou, M. Cococcioni, K. Kang, G. Ceder, Electrochemistry Communications 6 (2004) 1144.
[27] F. Zhou, M. Cococcioni, C.A. Marianetti, D. Morgan, G. Ceder, Physical Review B 70 (2004) 235121.
[28] X. Jiang, G.Y. Guo, Physical Review B 69 (2004) 1551108.
[29] H. Jonsson, G. Mills, K.W. Jacobsen, in: B.J. Berne, G. Ciccotti, D.F. Coker (Eds.), Classical and Quantum Dynamics in Condensed Phased Simulations, World Scientific, River Edge, NJ, 1998, p. 385.
[30] G. Henkelman, H.J. Jonsson, Chemical Physics 113 (2000) 9978.
[31] D. Su, H. Ahn, G. Wang, Applied Physics Letters 99 (2011) 141909.
[32] G.H. Vineyard, Journal of Physics and Chemistry of Solids 3 (1957) 121.
[33] K. Kang, D. Morgan, G. Ceder, Physical Review B 79 (2009) 014305.